R-21-oc

The Johns Hopkins University
APPLIED PHYSICS LABORATORY
Silver Spring, Maryland

TS-1125
Enclosure (2)

SIP-86-65
October 1965

Satellite 1963 38C

I. Introduction

Satellite 1963 38C was designed and built by the Applied Physics Laboratory of the Johns Hopkins University. The purpose of this document is to describe the satellite and, in particular, its complement of charged particle detectors in sufficient detail that interested scientists can make use of data which have been transferred to the NASA Space Sciences Data Center at Goddard Space Flight Center. The satellite has now been operating over two years, and during this period there have been several occasions when, for one reason or another, some of the data have been unreliable. In the following sections we will try to point out some of these occasions and to explain them when possible. However, it is hoped that anyone wishing to use these data will become thoroughly familiar with the instruments and their "normal" behavior in different regions of space and will not attempt to use isolated data points. This is important because the data have not been edited, nor can we guarantee that all possible difficulties have been discovered.

II. General Information - 1963 38C

Launch Time: 2022 UT, 28 September 1963

Launch Site: Vandenberg AFB, California

Initial Orbit: 28 September 1963

Semimajor axis	1.17312 earth radii*
Eccentricity	0.00311

Inclination	89.94 degrees
Time of Perigee	82.254 kiloseconds
Argument of Perigee	279.998 degrees
Longitude of Ascending Node	12.523 degrees
Apogee Altitude	608 nautical miles
Perigee Altitude	583 nautical miles
Period	107.3 minutes

*1 earth radius $\approx$ 3443 nautical miles

Note: The earth's motion about the sun produces an apparent precession of the orbit plane with respect to the earth-sun line of about one degree per day in a westerly direction. The orbit plane contained the earth-sun line on 4 October 1963.

Satellite Characteristics: A diagrammatic view of the satellite is shown in Figure 1.

Weight: 135 pounds

Power Supply: Solar cells on four blades and Ni-Cd batteries.

Transmissions:

A. Doppler Transmitters (for tracking)
   1. 162 Mh, 0.250 watts
   2. 324 Mh, 0.500 watts

B. Telemetry
   r-f carrier - 136.650 Mh, 0.750 watts. The carrier is phase modulated by each of 2 subcarrier

oscillators (maximum excursion ± 1 radian)

1. 10.5 kh SCO - carries digital information at the rate of 195.3 bits/second using an NRZ code with low band edge representing a digital zero and high band edge a digital one. ± 6% frequency deviation is used.
2. 5.4 kh SCO - pulse amplitude modulated to ± 6% frequency deviation to carry information from one of two 35 channel commutators. Commutation cycle is ~ 25 seconds. Minimum dwell time on any one function is 0.48 seconds.

Attitude Stabilization:

The spacecraft is magnetically stabilized by a cylindrical bar magnet with a dipole moment of 9.6×10^4 pole-cm parallel to the symmetry (Z) axis of the satellite. The period of oscillation in a field of 0.315 gauss is 7.36 minutes. Four magnetic hysteresis rods are installed in the solar cell blades to provide spin and oscillation damping. The amplitude of the residual oscillations is latitude dependent, being larger at the equator, and has been typically less than 6°. The measured angle between the field and

the alignment axis during a pass three days after launch is shown in Fig. 2.

Attitude Determination:

A three-axis flux gate magnetometer system is used to measure the deviation of the alignment axis from the field direction. No azimuthal measurements are made.

III. Telemetry and Data Systems

A detailed description of the satellite telemetry system and the data processing system is of no particular value since only data from the charged particle detectors and relevant auxiliary data are contained on Dictionary II tapes. The following is therefore limited to the aspects of the system which are directly pertinent to the use of the particle detector data.

A. Satellite Telemetry System

The satellite digital encoder contains a synchronizing word generator (16 bits), a frame counter (16 bits), and 14 data registers of 16 bits each. The data registers serve both as accumulators (scalers) and shift registers (during the readout cycle). The encoder contents are shifted out sequentially and continuously. Although the basic message length (subframe) is 256 bits, there are 25 output lines from detectors and only 13 registers available. Therefore, 12 registers are time shared and a complete frame consists of 2 subframes (512 bits). The subframes are identified in the synchronizing word. The remaining data register is used for telltales (8 bits) and to count the output of an A/D converter used to digitize the

analogue functions from a 35-channel commutator. The frame counter increments in subframe A and repeats in subframe B. The cycle time for the frame counter is therefore ~ 1.73 days, but it can be used to verify timing over a much longer period by simply counting the "rollovers." Note: When the satellite is in the "solar only" mode, most of the instruments, including the frame counter, are inoperative during periods of darkness.

The satellite contains two 35-channel commutators. The output of #1 is normally digitized and read out as part of the digital message, one channel per subframe. Commutator #2 is normally read out in analogue form on a separate subcarrier at twice the rate of #1. However, the two commutators can be switched on command, and the analogue commutator can be stopped on any channel for continuous monitoring.

The sampling rate and accumulation time for each detector is as follows:

Detector		Sampling Rate	Acc. Time
Electron Spectrometer	(10 channels)	22.9 min^{-1}	1.23 sec
Proton Spectrometer 90°	(6 channels)	22.9 min^{-1}	0.82 sec
Proton Spectrometer 180°	(6 channels)	22.9 min^{-1}	0.82 sec
Omnidirectional Detector A	(1 channel)	45.8 min^{-1}	1.23 sec
Omnidirectional Detectors B&C	(2 channels)	22.9 min^{-1}	1.23 sec

The auxiliary information which is normally presented with the data and sampling rate is given below.

Function	Sampling Rate
+ 6 v.	1.2 min^{-1}
- 6 v.	1.2 min^{-1}
Electron Detector Temp.	1.2 min^{-1}

Function	Sampling Rate
Omnidirectional Det. Temp.	1.2 min^{-1}
X-magnetometer	2.4 min^{-1}
Y-magnetometer	2.4 min^{-1}
Z-magnetometer	2.4 min^{-1}

B. Telemetry Station Network

The network of receiving stations which have supported 1963 38C are listed below. Not all of these stations have been active during the entire life of the spacecraft. The APL number is used to identify the stations on the data tapes.

APL No.	Location
003	Las Cruces, New Mexico
008	Sao Jose dos Campos, Brazil
014	Anchorage, Alaska
502	APL, Howard County, Maryland
510	South Point, Hawaii
542	Ascension Island
577	Salisbury, S. Rhodesia
667	Pretoria, S. Africa
764	Fort Myers, Florida
767	Quito, Ecuador
770	Santiago, Chile
775	College, Alaska
776	E. Grand Forks, Minnesota
777	Winkfield, England
779	Mojave, Cal.
780	Woomera, Australia

C. APL Data Processing System

In order to understand the data as presented in the Dictionary II format supplied to the Data Center, a brief description of the system is necessary.

Periodically, antenna pointing instructions are computed for all active receiving stations. The program computes instructions for all passes above the horizon for each station and assigns each pass a serial number. For each pass an IBM card is produced which contains pass serial no., satellite no., station no., day no., year risetime (UT), and sunlight indicator. The satellite number for 1963 38C is 63032. The statement concerning sun or shade refers to the risetime of the pass, i.e., the satellite may pass into or out of darkness during the pass. Since only a fraction of possible passes are observed, the pass serial numbers (in octal) on Dictionary II are not consecutive and may have large gaps.

When raw data from the stations arrives at APL, the passes are matched with their serial numbers and sent to the Pulse Data Processor (PDP). The PDP performs the following functions: (1) supplies header and pass identification information, (2) for digital information, makes positive "1" or "0" bit identification, (3) digitizes analogue data, (4) decodes station time and correlates it with the data, (5) indicates periods of noisy data. Considerable emphasis has been placed on the accurate correlation of time with the data. The time of the beginning of each subframe is generally determined to within $\sim$ 10 milliseconds and is used in the ephemeris computation. The time given in Dictionary II may be rounded to the nearest second.

The output of the PDP is run through a short program on the IBM 1401 computer in which the pass identification is checked against the cards produced in the preparation of antenna pointings. Additional header information

is supplied at this point including special time correlations for stations not equipped with automatic time code generators.

Following this step the tapes are processed through the Dictionary I program on the IBM 7094 computer. This program decommutates the digital message and organizes the data together with time, noise flags, etc., and prepares a listing and the Dictionary I output tape. The dictionary format in use at APL is a scheme of indirect addressing which eases programming and storage and retrieval problems. The Dictionary I tape is the basic raw data storage medium, and as such, is always duplicated, one copy serving as a working tape and the other as an archive copy. Note that the processing through Dictionary I has not purposely altered the raw data in any way. No corrections have been made. The raw data have simply been correlated with time and stored in an accessible format.

At this point, the data enter a complex of programs called Dictionary II. The particle detector data are converted from counts/frame to counts/second and corrected for instrument dead time; statistical uncertainties are computed; auxiliary data are converted to appropriate units of voltage, temperature, and magnetic field; orientation angles are computed; and the satellite ephemeris is correlated with the data. The ephemeris is derived from the Doppler tracking system developed at APL. Orbit determinations are made at intervals of 1 to 2 weeks and the Kepler elements are used in the Dictionary II program to generate the ephemeris. Satellite position is computed at the beginning of each full frame (i.e., at 2.62 second intervals) and McIlwain's program No. C3, as obtained from the Goddard Space Flight Center in 1962, is used to compute B and L for each position. The error in satellite position is estimated to be always less than 10 km, and generally much better, excluding occasional gross errors in timing. The error estimate includes the effect of interpolating between the

relatively infrequent sets of Kepler elements. The acceptable error is set by detector accumulation times ($\sim$ 1.2 sec) and satellite velocity ($\sim$ 8 km/sec). Estimates of errors in B and L have been discussed by McIlwain.*

A complete list of the information of interest to the user which is contained on a Dictionary II tape is given below. This is information for the user; format information for computer programming will be available at the Data Center.

1. Header Record - The header record appears at the beginning of each pass and contains the following information:
    a. Station number
    b. Satellite number
    c. Year
    d. Day number (UT)
    e. Pass risetime (UT)
    f. Sun or shade indicator
    g. Pass serial number
    h. Kepler orbit - epoch, semi-major axis, eccentricity, inclination, longitude of ascending node, argument or perigee, mean anomaly, precession of node, precession of perigee.
    i. Longitude of Greenwich at 0 hrs UT on the day of the data.

---

*C. E. McIlwain, "Practical B-L Space Model" presented at the Advanced Study Institute, "Radiation Trapped in the Earth's Magnetic Field," August 16 through September 3, 1965, Bergen, Norway.

2. Common Record - The common record appears once for each full frame of data (i.e., subframes A and B) and contains information which applies to that frame.

    a. Frame number

    b. Beginning time (in seconds UT) of subframe A (or B if A is missing).

    c. Latitude of satellite at above time in degrees.

    d. Longitude of satellite at above time in degrees.

    e. Altitude of satellite at above time in degrees.

    f. Magnetic field value at satellite position in gauss.

    g. L-value at satellite position in earth radii.

    h. Information word - indicates data which is absent or has been deleted, and the reasons.

3. Subframe A

    a. 90° proton spectrometer channel 1 corrected counting rate.

    b. 90° proton spectrometer channel 1 statistical uncertainty.

    c. " " " " 2 ccr

    d. " " " " " su

    e. " " " " 3 ccr

    f. " " " " " su

    g. " " " " 4 ccr

    h. " " " " " su

    i. " " " " 5 ccr

    j. " " " " " su

    k. " " " " 6 ccr

    l. " " " " " su

m. Omnidirectional detector A ccr

n. Omnidirectional detector A su

o. Electron spectrometer channel 1 ccr

p. " " " " su

q. " " " 2 ccr

r. " " " " su

s. " " " 3 ccr

t. " " " " su

u. " " " 6 ccr

v. " " " " su

w. " " " 7 ccr

x. " " " " su

y. " " " 8 ccr

z. " " " " su

4. Subframe B

a. 180° proton spectrometer channel 1 ccr

b. " " " " " su

c. " " " " 2 ccr

d. " " " " " su

e. " " " " 3 ccr

f. " " " " " su

g. " " " " 4 ccr

h. " " " " " su

i. " " " " 5 ccr

j. " " " " " su

k. 180° proton spectrometer channel 6 ccr

l. " " " " " su

m. Omnidirectional detector A ccr

n. " " " su

o. " " B ccr

p. " " " su

q. " " C ccr

r. " " " su

s. Electron spectrometer channel 4 ccr

t. " " " " su

u. " " " 5 ccr

v. " " " " su

w. " " " 9 ccr

x. " " " " su

y. " " " 10 ccr

z. " " " " su

5. Commutator record - The commutator record appears periodically through the pass and contains the following information:

a. time of magnetometer data

b. X-magnetometer in gauss

c. Y-magnetometer in gauss

d. Z-magnetometer in gauss

e. $(X^2 + Y^2 + Z^2)^{1/2}$ = B measured

f. B measured/B calculated

g. alpha - angle between Z axis and $\bar{B}$ (degrees)

h. beta - angle between electron spectrometer (and 90° proton spectrometer) and $\vec{B}$ (degrees)

i. electron detector temperature (degrees F.)

j. Omnidirectional detector temperature (degrees F.)

k. + 6 v. line

l. - 6 v. line

In the preceding list "corrected counting rate" (ccr) means that the raw counts/frame (C) have been converted to counts/sec (N) and corrected for instrument dead time. The dead time correction is

$$ccr = \frac{N}{1 - N\rho}$$

where $\rho = 10\mu s$ for the electron spectrometer and omnidirectional detectors, and $\rho = 13\mu s$ for the proton spectrometer.

The statistical uncertainty (su) is obtained simply by assuming Poisson statistics apply, i.e.,

$$su = \frac{ccr}{\sqrt{C}} \quad .$$

Detector channels are explained in the next section.

IV. Charged Particle Experiments

Satellite 1963 38C contains an integral electron spectrometer, a differential proton spectrometer, and a set of omnidirectional detectors. All of these instruments utilize solid state detectors, and they are described in detail below.

A. Integral Electron Spectrometer

Five 1000μ surface barrier solid state detectors make up the electron spectrometer. These units are mounted in ceramic ring transmission

mounts and are biased to full depletion. While full depletion occurs at ~ 160 volts, a bias voltage of 200 volts is used to ensure full depletion across the area of the detector.

The detectors, the various foils used and the two discriminator levels of 250 kev and 1 Mev (used as a single-channel analyzer) yield the particle response characteristics shown in Table 1. Also shown are various pertinent parameters of each detecting channel.

Each detector has its own preamp-amplifier-discriminator combination, all of which were chosen on the basis of similar temperature-voltage characteristics. Except for its look angle, each detector is shielded by a minimum of 5.7 gms/cm^2 of Cu shielding which represents the range of ~ 65 Mev protons and ~ 11 Mev electrons. Figure 3 shows a view of one of the detectors in its housing.

From Table 1 we see that events lying between the two discriminator levels will be mainly due to electrons, the proton contribution being negligible. Detectors 1 and 5 were chosen to have similar energy response and different geometric factors in order to obtain an estimate of the omnidirectional background which would stem from penetrating particles and possible bremsstrahlung. Above L ~ 2 inspection of detector 4 has proved to be a much handier method of estimating the importance of this possible background contamination.

All detectors were calibrated by obtaining their electron detection efficiency when connected to flight electronics, i.e., the ratio of the number of electrons yielding pulses lying between the two discriminator levels to the total number of electrons incident on the detector was obtained as a function of electron energy. Monoenergetic electron beams up to 1.8 Mev were obtained from a beta-ray spectrometer.

TABLE 1. Electron Spectrometer Characteristics: Oriented 90° to Satellite Alignment Axis

Detector	Half Angle (deg)	Geometric Factor (cm^2 ster)	Foil Thickness (mg/cm^2)	Particle Energies yielding pulses between 250 kev and 1 Mev discriminator levels		
				Electrons*	Protons (energies in Mev)	
1	6.4	$2.8(10)^{-3}$	10.3 AL	$\geq$ 0.28 Mev	$2.0 \leq E_p \leq 2.3$	$E_p \geq 178$ Mev
2	6.4	$2.8(10)^{-3}$	412 Cu	$\geq$ 1.2 Mev	$14.4 \leq E_p \leq 14.5$	$E_p \geq 179$
3	6.4	$2.8(10)^{-3}$	946 Cu	$\geq$ 2.4 Mev	$23.27 \leq E_p \leq 23.34$	$E_p \geq 181$
4	6.4	$2.8(10)^{-3}$	1470 Cu	$\geq$ 3.6 Mev	$30.01 \leq E_p \leq 30.07$	$E_p \geq 183$
5	3.2	$4.9(10)^{-4}$	10.3 AL	$\geq$ 0.28 Mev	$2.0 \leq E_p \leq 2.3$	$E_p \geq 178$

*All electron ranges and equivalent energies given in this paper are based on the range-energy data in Katz and Penfold, 1952. It is important to note that these are 10% transmission ranges and equivalent energies.

The resultant efficiency curve is shown in Figure 4. All detectors were found to have an energy response within 10% of this curve. Consequently, Figure 4 is used as the nominal response curve for these detectors.

It is seen that the efficiency rapidly rises to a maximum of ~ 0.95, remains approximately constant at this maximum value until ~ 800 kev, and then monotonically decreases to a value of 0.7. The maximum efficiency is limited to 0.95 due to backscattering events, in which the electrons deposit less than 250 kev in the detector.

There are two effects which lower the efficiency above ~ 800 kev; (1) above the penetration energy (670 kev) the most probable energy loss in the detector, $(\Delta E)_{prob}$, decreases with increasing electron energy, reaching a minimum of ~ 300 kev at 1.5 Mev. This coupled with an observed full width at half maximum of ~ 120 kev in the $(\Delta E)_{prob}$ peak, shows that some electrons will deposit less than 250 kev in the detector and thus not be counted; (2) there remains a significant probability that an electron of energy > 1 Mev will deposit > 1 Mev in the detector and thus not be counted as an electron. Figure 5 graphically shows the above effects taking place. The curves shown are typical spectrums taken with a 1000μ detector.

Electrons of energy > 1.8 Mev were not available to us. We have thus assumed the efficiency to remain constant at a value of 0.7 for all energies above 1.8 Mev. This is indicated by the dashed portion of the curve in Figure 4. The data do indeed show a leveling off at a value of 0.7 at energies $\gtrsim 1.5$ Mev. The leveling off of the efficiency in the range 1.5 - 2.0 Mev is expected, as is a slight increase in efficiency at higher energies. This is due to the decreasing probability of depositing $\geq$ 1 Mev in the detector

with increasing energy and to the increase in $(\Delta E)_{prob}$ above 2.0 Mev. In lieu of experimental data above 2.0 Mev, we have assumed the constant value of 0.7.

The shape of the efficiency curve discussed above will be affected by the presence of shielding foils placed in front of the detectors. Figure 6 shows the result of combining the measured efficiency curve of a particular detector with the transmission probability curves [Birkhoff, 1958] for the 10.3 mg/cm^2 Al and 412 mg/cm^2 Cu foils. Also shown are the experimental values obtained with the foils in place. The agreement is quite good for the 10.3 mg/cm^2 foil mainly because these foils may be considered "thin" for all energies pertinent to the experiment. This is not the case with the thicker foils used in the higher energy channels. In Figure 6 we see that for the 412 mg/cm^2 foil the experimental values are initially higher and subsequently lower than the predicted values. This can be explained by the fact that an average energy loss in the foil was used to obtain the electron energy on the exit side of the foil. This was done since the transmission curves give only the fractional transmission through a foil and yield no information concerning the angular and energy distributions of the emerging electrons. Ignoring these distributions and using an average energy after the foil causes the predicted value to behave as in Figure 6 when a threshold effect is being measured. At higher energies, where the foil may be considered "thin", the predicted and measured values should agree as they do for the 10.3 mg/cm^2 foils.

The predicted efficiency curves with the foils in place, obtained from the nominal measured response curve of Figure 4, are shown in Figure 7. For consistency these predicted efficiencies are used when converting from observed count rates to flux values. In channels 2, 3, and 4, these efficiencies are upper limits and depending on the assumed spectrum can yield an error in the absolute flux of as much as 25%. The error in channel 1 will be $\lesssim$ 15%.

A detailed study of the response of this instrument to penetrating protons in the inner Van Allen belt is currently under way. It will be published in the near future as part of a paper on the decay of the artificial belt by the authors (not necessarily in order) C. O. Bostrom, D. S. Beall, and D. J. Williams.

The channel numbers referred to in Section III.C are identified as follows: Channels 1 to 5 are the "window" counting rates for detectors 1 to 5 given in Table 1. Channels 6 to 10 are the upper level counting rates for detectors 1 to 5 respectively. In other words, the total counting rate for detector D_i is the sum $(C_i + C_{i+5})$.

B. Proton Spectrometer

The proton spectrometer consists of two solid state radiation detectors located as shown in Figure 8. Each is of the silicon surface barrier type, 500 microns thick and fully depleted. The several energy ranges (and certain background measurements) are obtained by observing the detector outputs both singly and in coincidence as shown in the following table:

Channel	Energy Range	Mode of Operation
1	1.2 - 2.2 Mev	$A\bar{B}$
2	2.2 - 8.5 Mev	$A\bar{B}$
3	8.5 - 25 Mev	AB
4	25 - 100 Mev	AB
5	Channel 1 background	$\bar{A}B$
6	Channel 2 background	$\bar{A}B$

The above energy ranges are all obtained by setting discrimination levels at 0.7, 2.0, and 8.5 Mev on both detectors and appropriately combining their

outputs. The upper level discriminator eliminates counts from those heavier charged particles which would deposit more than 8.5 Mev in the detector, and also counts from protons in a limited energy range which penetrate the shielding and, because of greater path length in the detector, deposit more than 8.5 Mev.

The details of the detection system may be best understood by reference to Figure 9, which shows the amount of energy deposited (pulse height) in each detector as a function of incident proton energy. Particles are considered as incident normal to detector A.

Channels 1 and 2: Protons of energy less than 1.2 Mev will not be counted since they cannot pass through the aluminized mylar light shield and trigger the lower level discriminator at the output of detector A. Protons in the energy interval 1.2 Mev to $\sim$ 8.0 Mev stop in detector A, trigger the proper discriminators, and are counted in channel 1 or 2. In each case an $A\bar{B}$ anticoincidence is required.

Channel 3: Protons in the interval 8.5-25 Mev will pass completely through detector A, depositing between 8.5 and 2.0 Mev in it, and further will leave between > 0.7 Mev in detector B. An AB coincidence involving the 2.0-8.5 Mev range in A is required.

Channel 4: Protons in the interval 25-100 Mev will pass completely through detector A, depositing between 2.0 and 0.7 Mev in it, and further will leave > 0.7 Mev in detector B. An AB coincidence involving the 0.7-2.0 Mev range in A is required. The upper energy limit of 100 Mev is somewhat fuzzy because pulse height changes slowly with energy in this region. Protons of energy greater than 100 Mev will leave less than 0.7 Mev in both detectors and not register. The proper operation of the device requires that detector B be no thinner than detector A.

Channels 5 and 6: Since detectors A and B have similar shielding, monitoring the singles rates in the 0.7-2.0 Mev and 2.0-8.5 Mev ranges of detector B (using $\bar{A}B$ anticoincidences) will give background counting rates due to penetrating particles that can then be used to correct Channels 1 and 2. Some care must be used because the shielding is not identical and a 1 for 1 subtraction is often not permissible.

In addition to the background monitoring done by Channels 5 and 6, several other forms of background must be considered:

1. Accidental coincidences between detectors A and B leading to false counts in Channel 3 and 4 can be calculated from the A and B singles rates and the circuit resolving time. The A singles rate is given by the sum of Channels 1, 2, 3, and 4, and the B singles rate is the sum of Channels 3, 4, 5, and 6. The coincidence resolving time is 4×10^{-7} sec.

2. True AB coincidences will occur due to penetrating particles passing backwards through the system, i.e., in the B-A direction. The use of ~ 12 g/cm^2 of copper (100 Mev proton range) behind detector B will reduce the background in Channel 3 to particles in the range 100.83 to 105.5 Mev and in Channel 4 to particles in the ranges 100.76 to 100.83 and 105.5 to 198.7 Mev. Here only the range 105.5 to 198.7 Mev is wide enough to contain any appreciable number of particles, and it will therefore weight Channel 4 (25-100 Mev) somewhat toward the high end. Since the number-energy spectrum falls off rapidly with energy, this is not usually serious.

3. Low energy electrons are prevented from entering detector A, where pile-up might produce false pulses, by a sweeping magnet in front of this detector.

4. Most high energy (minimum ionizing) electrons incident normal to detector A will deposit only $\sim$ 200 kev energy in each detector, less than the 700 kev threshold. However, there is a background contribution to the counting rate of channel 1 because of the finite probability that a high energy electron will deposit more than 700 kev in detector A. The efficiency for this process has been measured and found to rise sharply to a maximum of 9% at 800 kev, and fall rapidly to < 2% at 1.8 Mev incident electron energy. Channel 5 (detector B) has a similar, but much smaller, contribution.

1963 38C contains two proton spectrometers, one with its axis normal to the magnetic field line ($\varphi = 90°$) and one with its axis parallel ($\varphi = 180°$) to the field line. Note that $\varphi = 180°$ means that the spectrometer "looks" away from the earth in the northern hemisphere. The two detector assemblies share common electronics following preamplification and are commutated so that the 90° unit is read in subframe A and the 180° unit in subframe B.

The channel numbers used above correspond to those given in Section III.C.

C. Omnidirectional Detectors

The omnidirectional detectors on 1963 38C consist of three lithium-drifted silicon solid state detectors, each being a cube about 1.4

mm on a side. They protrude through the satellite skin and have an unobstructed field of view over 2π sterradians. The energy thresholds are set primarily by hemispherical aluminum absorbers. Each detector has its own preamplifier, amplifier, and integral discriminator. The discriminator level is set at 250 kev for all detectors and when this is combined with the absorber thicknesses, we get energy thresholds for protons and electrons as given below:

Detector	Electrons	Protons	Geometric Area Factor
A	> 0.28 Mev	> 2.2 Mev	~ 0.03 cm^2
B	> 0.41 Mev	> 8.5 Mev	~ 0.03 cm^2
C	> 1.8 Mev	> 25 Mev	~ 0.03 cm^2

V. General Considerations

The 1963 38C telemetry system is overdesigned from the viewpoint of transmitter power and as a result the data are usually very clean and very little has to be discarded. There have been various payload and instrument problems arise, however, and although most of these have been temporary we will attempt to enumerate those of which one should be aware in using the data.

A. Spacecraft Problems

As mentioned previously with regard to the frame counter, the satellite can be commanded to either a "battery" or "solar only" mode. In the solar only mode, almost all satellite systems are inoperative in the dark. However, even in sunlight the satellite may assume an attitude with respect to the sun in which insufficient power is generated by the solar cells, resulting in a decrease in voltages. It is, therefore, recommended that the + 6 and - 6 v.

lines be checked before using the data. This condition may persist for only one to several minutes but definitely affects observed counting rates.

Early in its life the satellite temperature rose to an excessively high value. During these periods several of the solid state detectors became noisy and subsequently recovered when the temperature dropped. Caution is urged whenever the detector temperatures exceed 100° to 110°F.

The 162 mc/s Doppler transmitter failed in April 1964 and because of the power unbalance the satellite has been in "solar only" since then. The 324 mc/s transmitter is still functioning properly and the failure had no serious effect on the satellite tracking because of the relatively crude information required.

B. Instrument Problems

To the best of our knowledge, there has been only one detector failure of the 12 solid state detectors used in 1963 38C. Detector number 4 of the electron spectrometer ($E_e \geq 3.6$ Mev) has been intermittently noisy since early December, 1963 and for most of the time periods examined, has been unusable. There are isolated periods when the detector is quiet and can be used but it is not recommended unless great care is taken.

The electron spectrometer channels 1 and 5 nominally differ only in directional geometric factor. However, because of the construction of the collimators, the expected counting rate ratio turns out to be somewhat spectrum dependent. Details are too complex to be discussed here, but in a hard spectrum like the artificial zone, the effective geometric factor for C5 is larger than that given in Table 1.

The proton spectrometer experienced an intermittent failure in the logic several times during the first month in orbit for periods of as much as a day. The cause is unknown but the symptom is loss of channels 2 and 3 (i.e., all zero counts). The failure is obvious for passes through the inner zone, but not at all apparent at high latitudes. To our knowledge, this failure has not reoccurred since October, 1963. There are no known cases of malfunction of any of the omnidirectional detectors.

We have no indication that any of the detectors or the associated electronics have suffered any long term degradation or drift over the first two years of satellite life. Since we do not have in-flight calibration, the above statement is based on consistent behavior of the instruments in regions of space where little change is expected.

The flux-gate magnetometers apparently suffer from calibration uncertainties as evidenced by the ratio B measured/B calculated. It is believed that most of the trouble is due to zero offset and therefore the computed angles may be incorrect, but the excursion indicated should be reliable. On at least one (June 1964) and possibly several occasions, the satellite oscillations about the field line increased in amplitude to $> 10^{\circ}$ for some mysterious reason. One result of a large amplitude oscillation is to introduce excessive scatter in the measurements of trapped radiation.

C. Other Problems

An erroneous ephemeris can be the result of timing errors, either in the receiving stations or in the data processing, or from human and computer errors in generating Kepler elements. All of the above errors have occurred (infrequently), and we believe that all have been found. However, there may be isolated passes which are wrong and have not been corrected.

Although the above list of problems may appear long, two things should be kept in mind. First, most of the problems enumerated are infrequent, or isolated to one detector and/or time period. Second, most can be readily detected by anyone who is familiar with the data. We, therefore, repeat the statement made in the introduction that anyone wishing to use the data should take the time to become familiar with the instruments and their behavior.

For further information please contact the Project Scientist, Dr. Carl O. Bostrom, The Applied Physics Laboratory, The Johns Hopkins University, 8621 Georgia Avenue, Silver Spring, Maryland, telephone no. 776-7100, x 2066.

FIGURE CAPTIONS

1. Diagramatic view of satellite 1963 38C.

2. Alignment of satellite 1963 38C three days after launch. The maximum and minimum values of β are $90 \pm \alpha$ degrees. Where and when this occurs is a function of satellite rotation and precession rates. The time variation shown above results from satellite nutation. The observed period of ~ 7.6 min. agrees well with a predicted period of 7.36 min. The maximum value of α is latitude dependent, being larger at the equator; and has been typically less than 6°.

3. Portion of electron spectrometer showing one of the five detectors in its housing.

4. Electron detection efficiency versus incident electron energy for a 1000μ surface barrier detector without shielding foils. Detection occurs if an output pulse lies between the 250 kev and 1 Mev discrimination levels.

5. Distributions of ΔE in a 1000μ surface barrier detector for various incident electron energies.

6. Electron detection efficiency versus incident electron energy for a 1000μ surface barrier detector with indicated shielding foils in place. The solid line is the predicted curve. Points are experimental values.

7. Predicted electron detection efficiencies versus incident electron energy for the four shielding foils used in the electron spectrometer.

8. Proton Spectrometer, 1963 38C.

9. ΔE vs. E for Proton Spectrometer detectors A and B.

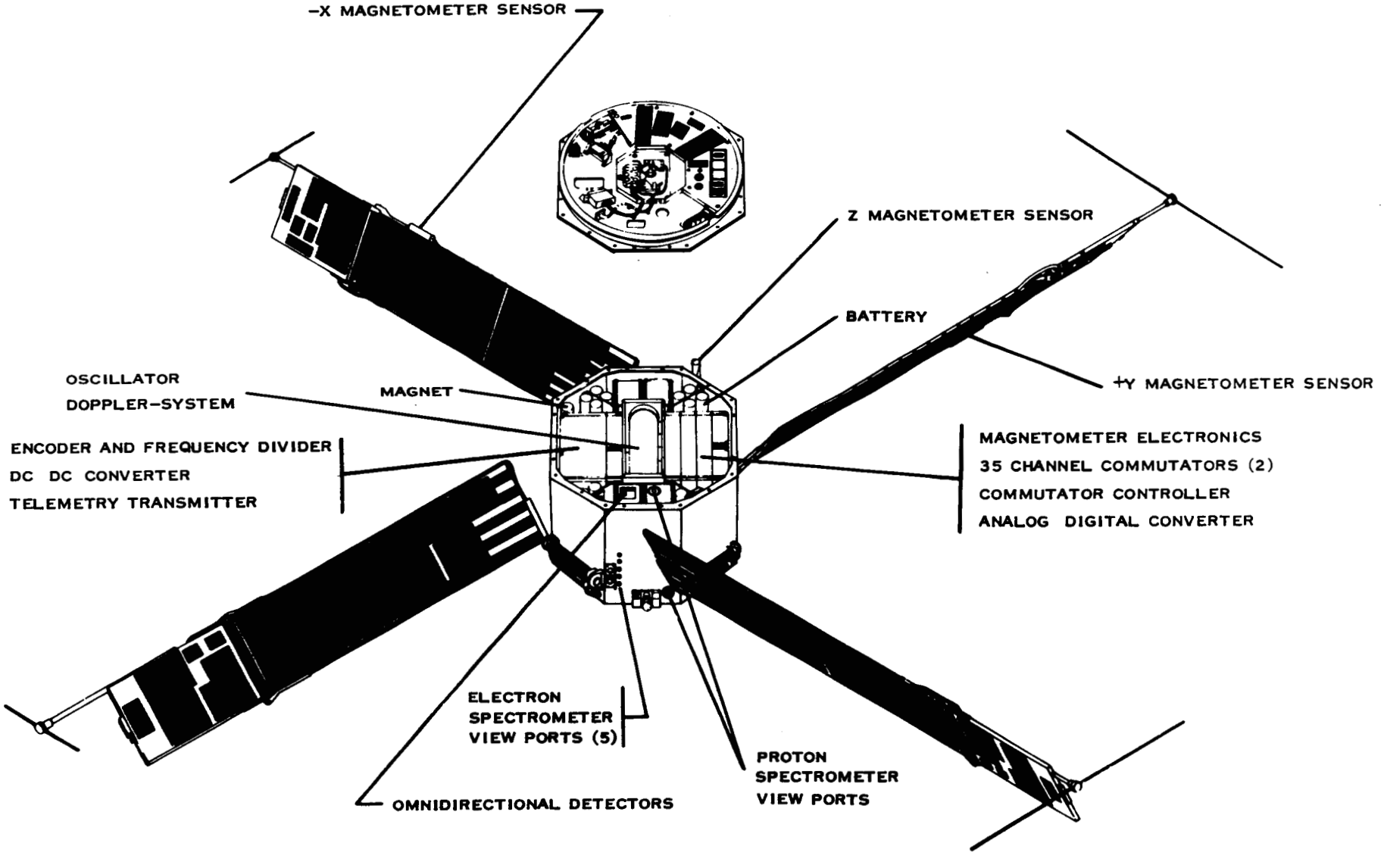

REV. AUGUST 1964

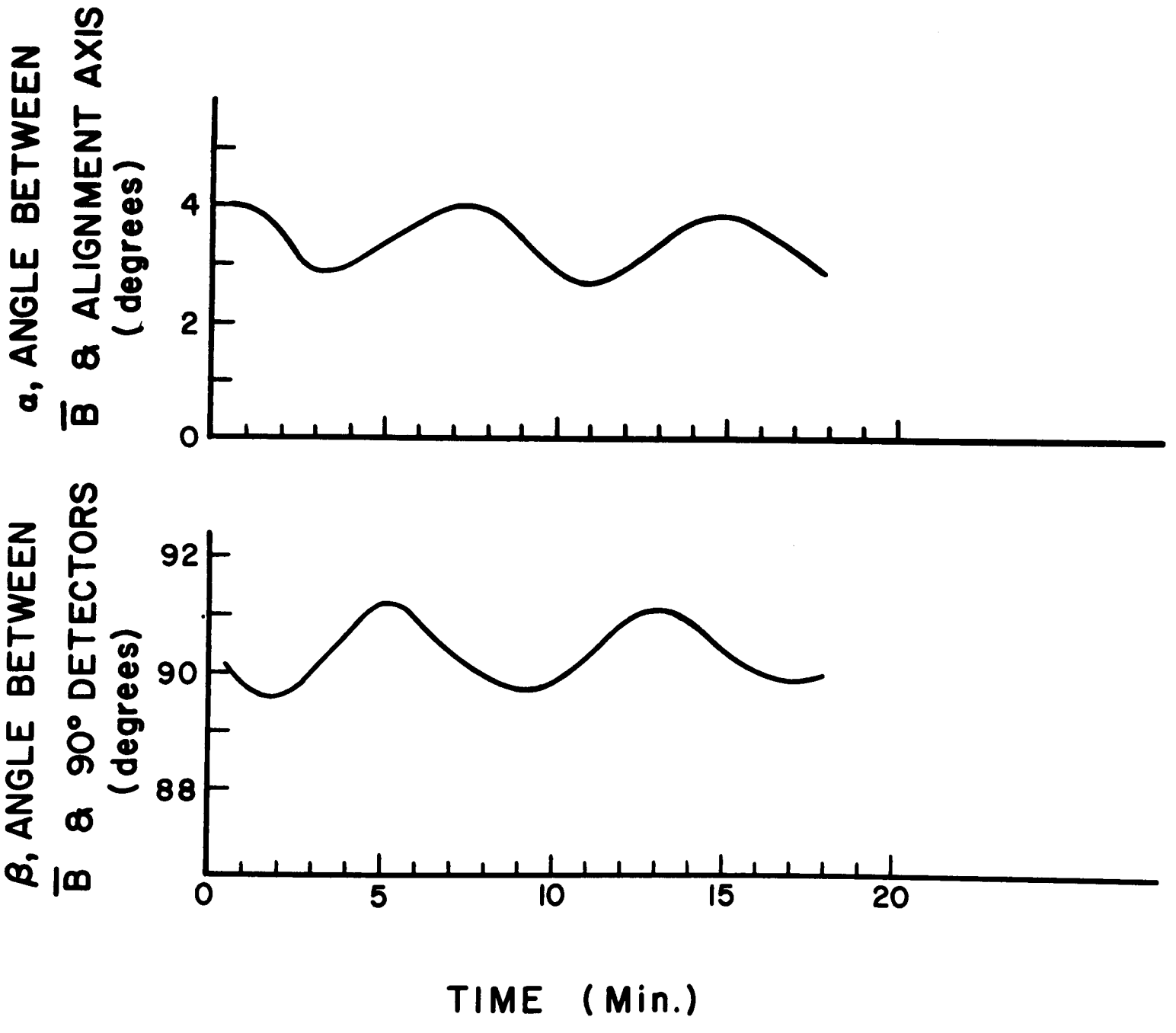
α, ANGLE BETWEEN B̄ & ALIGNMENT AXIS (degrees)
0
2
4
β, ANGLE BETWEEN B̄ & 90° DETECTORS (degrees)
88
90
92
0
5
10
15
20
TIME (Min.)

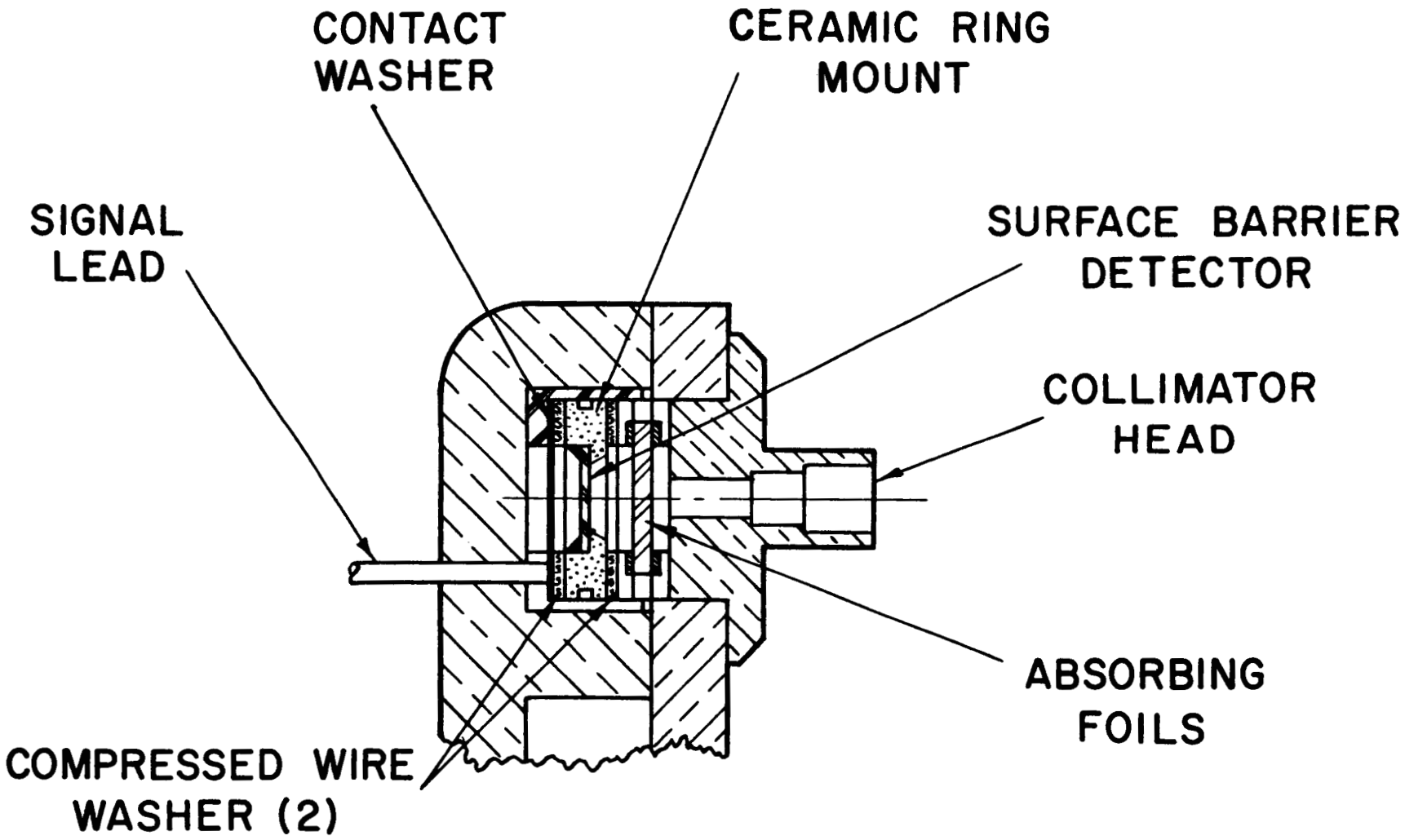
CONTACT WASHER
CERAMIC RING MOUNT
SIGNAL LEAD
SURFACE BARRIER DETECTOR
COLLIMATOR HEAD
ABSORBING FOILS
COMPRESSED WIRE WASHER (2)

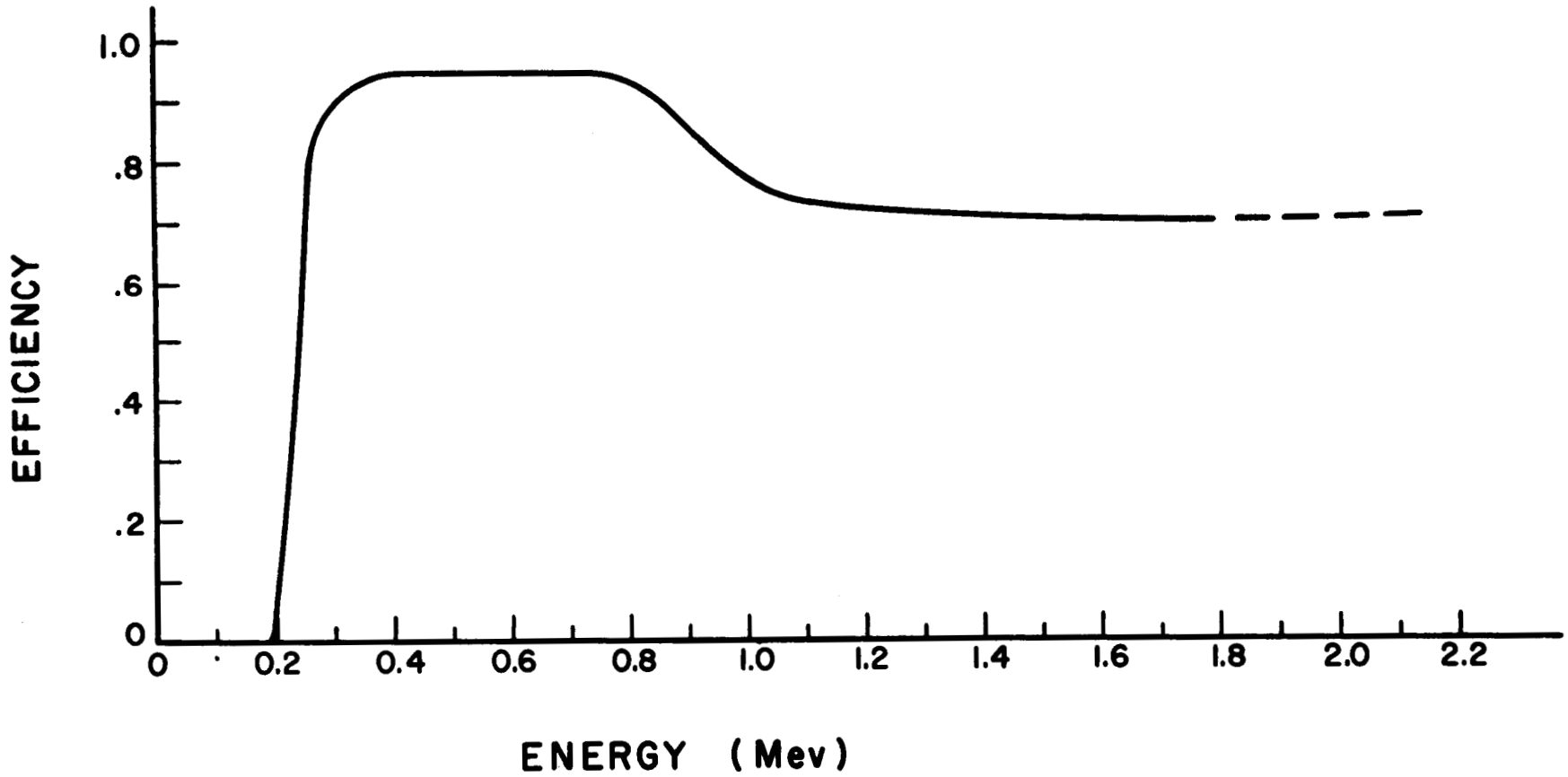
EFFICIENCY
1.0
.8
.6
.4
.2
0
0
0.2
0.4
0.6
0.8
1.0
1.2
1.4
1.6
1.8
2.0
2.2
ENERGY (Mev)

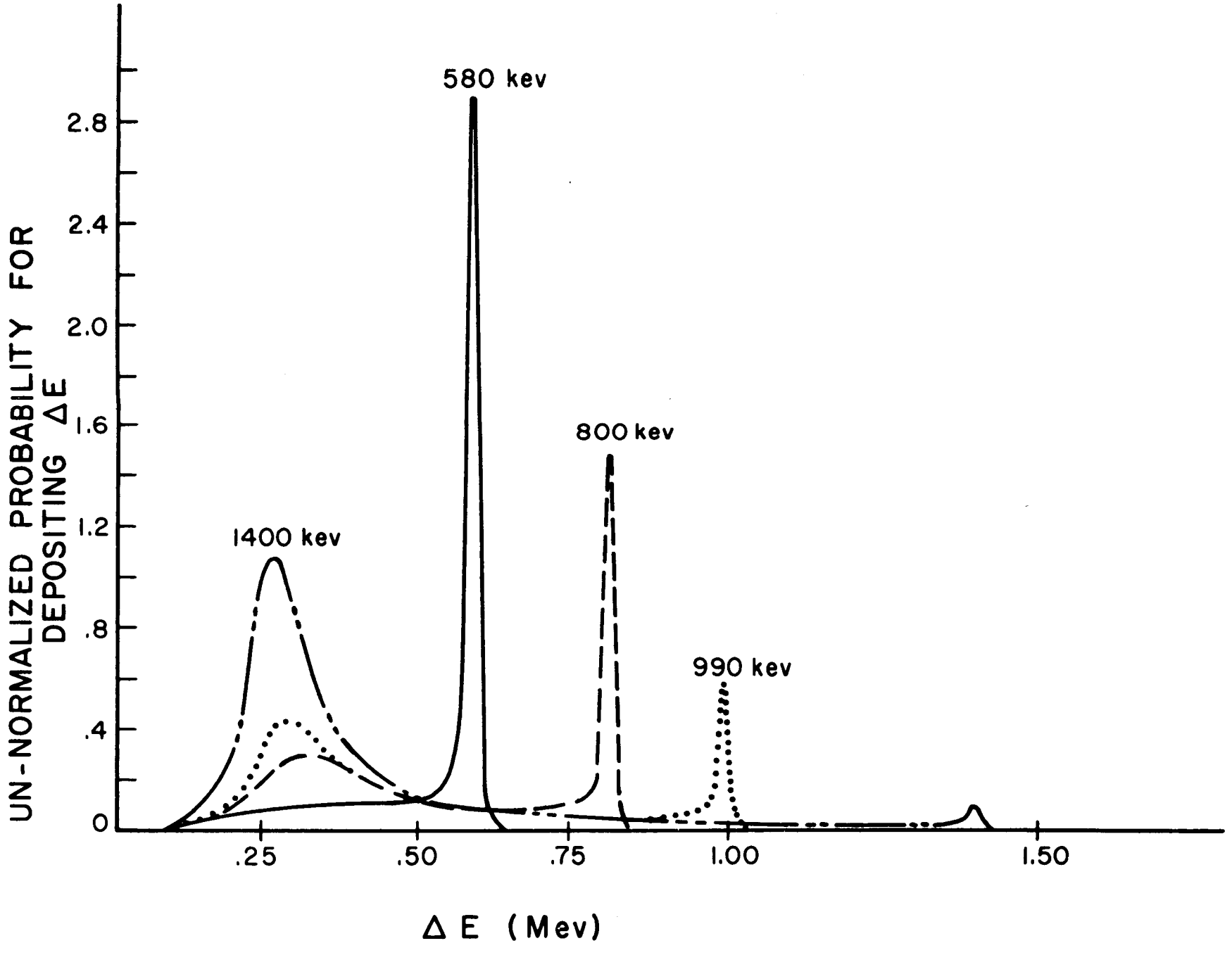
580 kev
800 kev
1400 kev
990 kev
UN-NORMALIZED PROBABILITY FOR DEPOSITING ΔE
2.8
2.4
2.0
1.6
1.2
.8
.4
0
.25
.50
.75
1.00
1.50
Δ E (Mev)

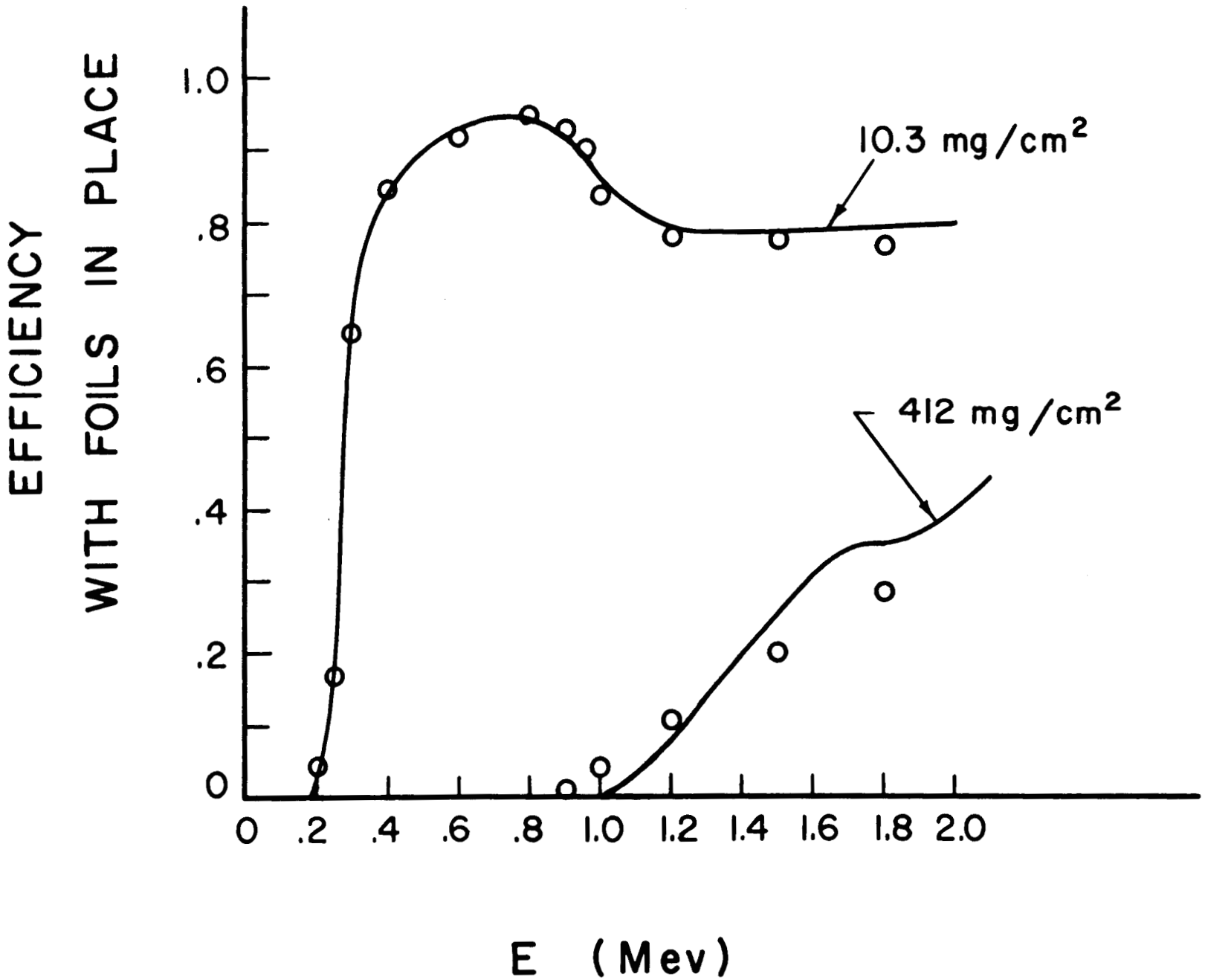
EFFICIENCY
WITH FOILS IN PLACE
1.0
.8
.6
.4
.2
0
10.3 mg/cm²
412 mg/cm²
0 .2 .4 .6 .8 1.0 1.2 1.4 1.6 1.8 2.0
E (Mev)

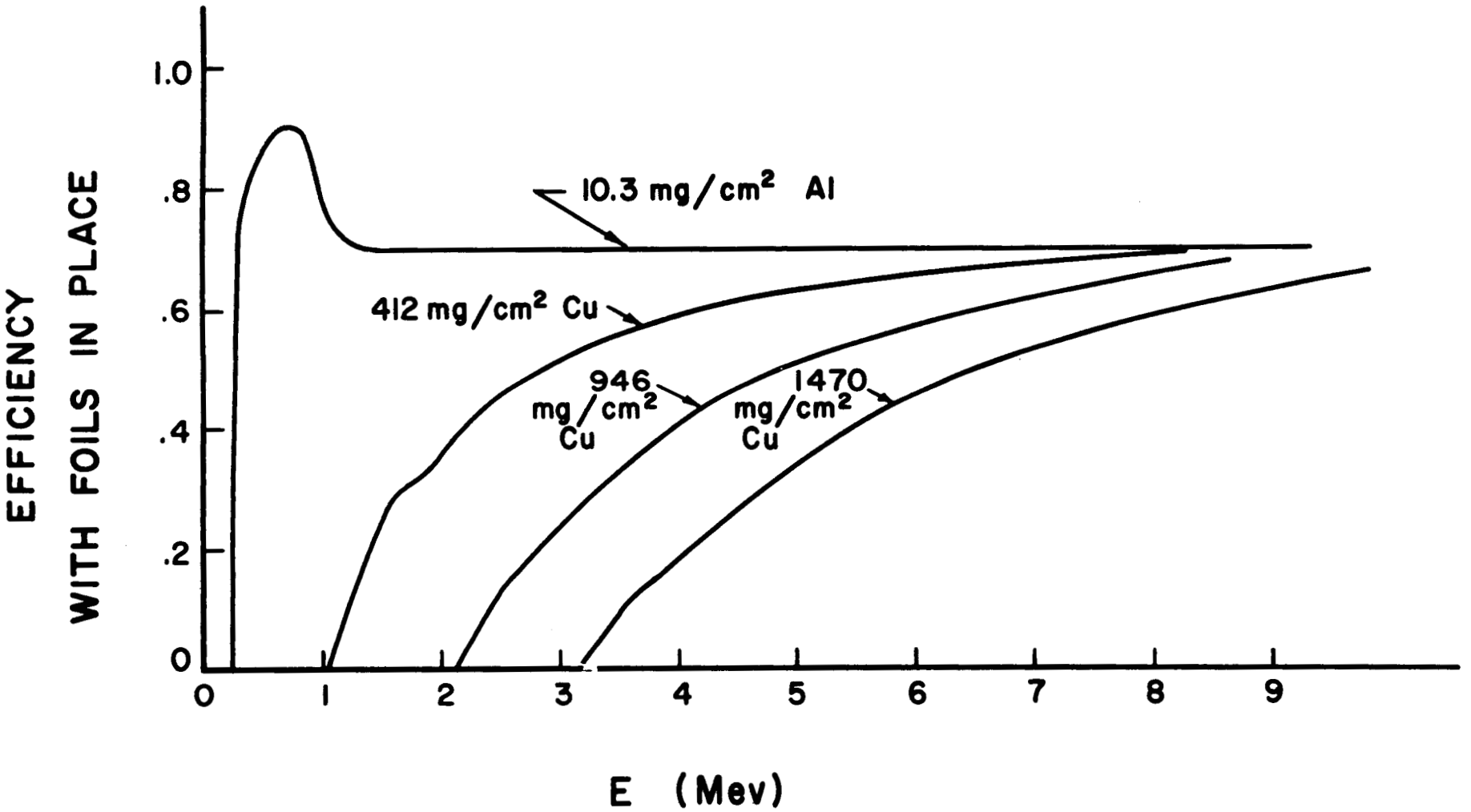
EFFICIENCY WITH FOILS IN PLACE
1.0
.8
.6
.4
.2
0
10.3 mg/cm² Al
412 mg/cm² Cu
946 mg/cm² Cu
1470 mg/cm² Cu
0
1
2
3
4
5
6
7
8
9
E (Mev)

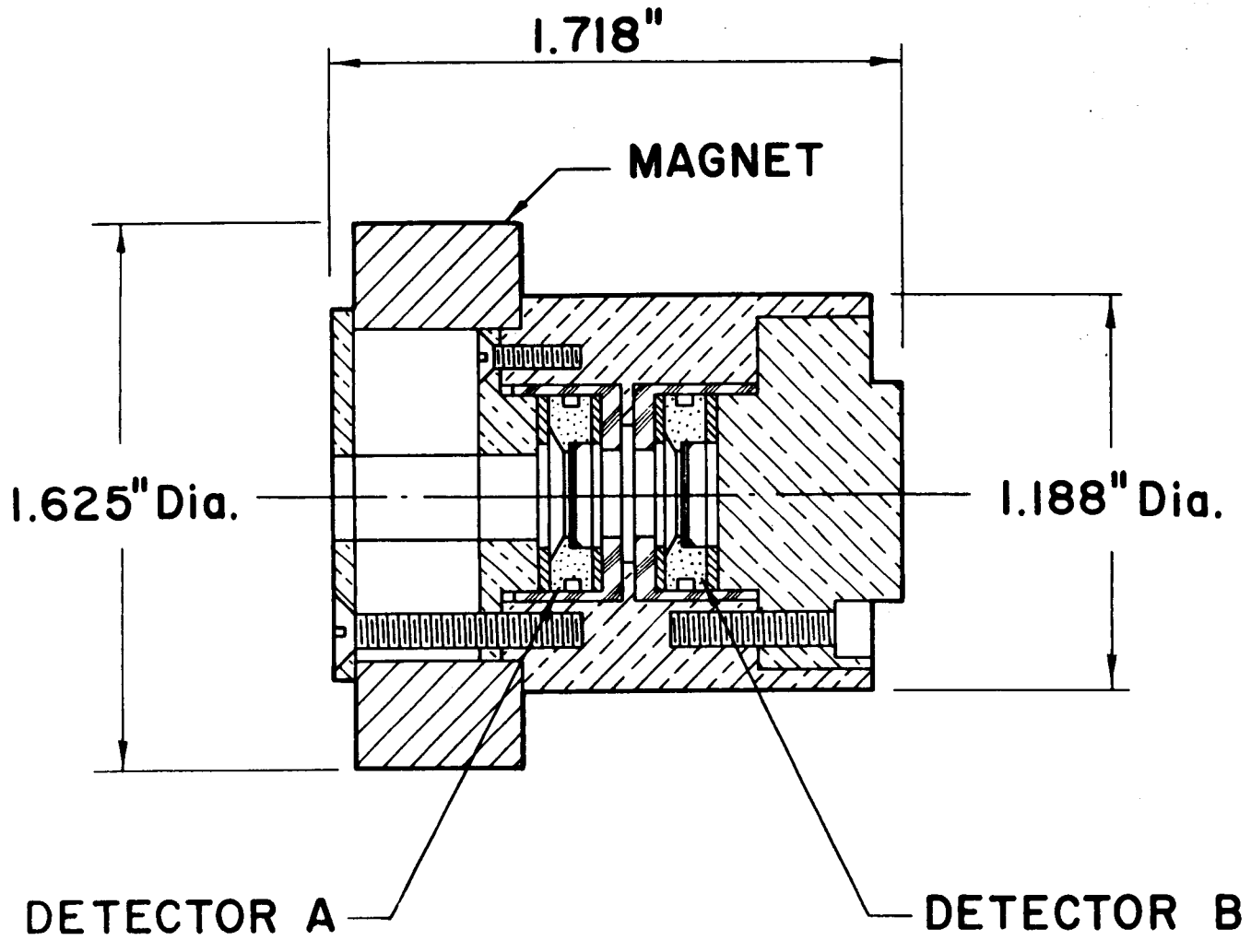

(Detectors surrounded by copper)

APL PROTON SPECTROMETER

Fig. 8

PROTON SPECTROMETER

Energy deposited in detectors A and B (each 500μ Si) for protons incident normally on A, as a function of proton energy.

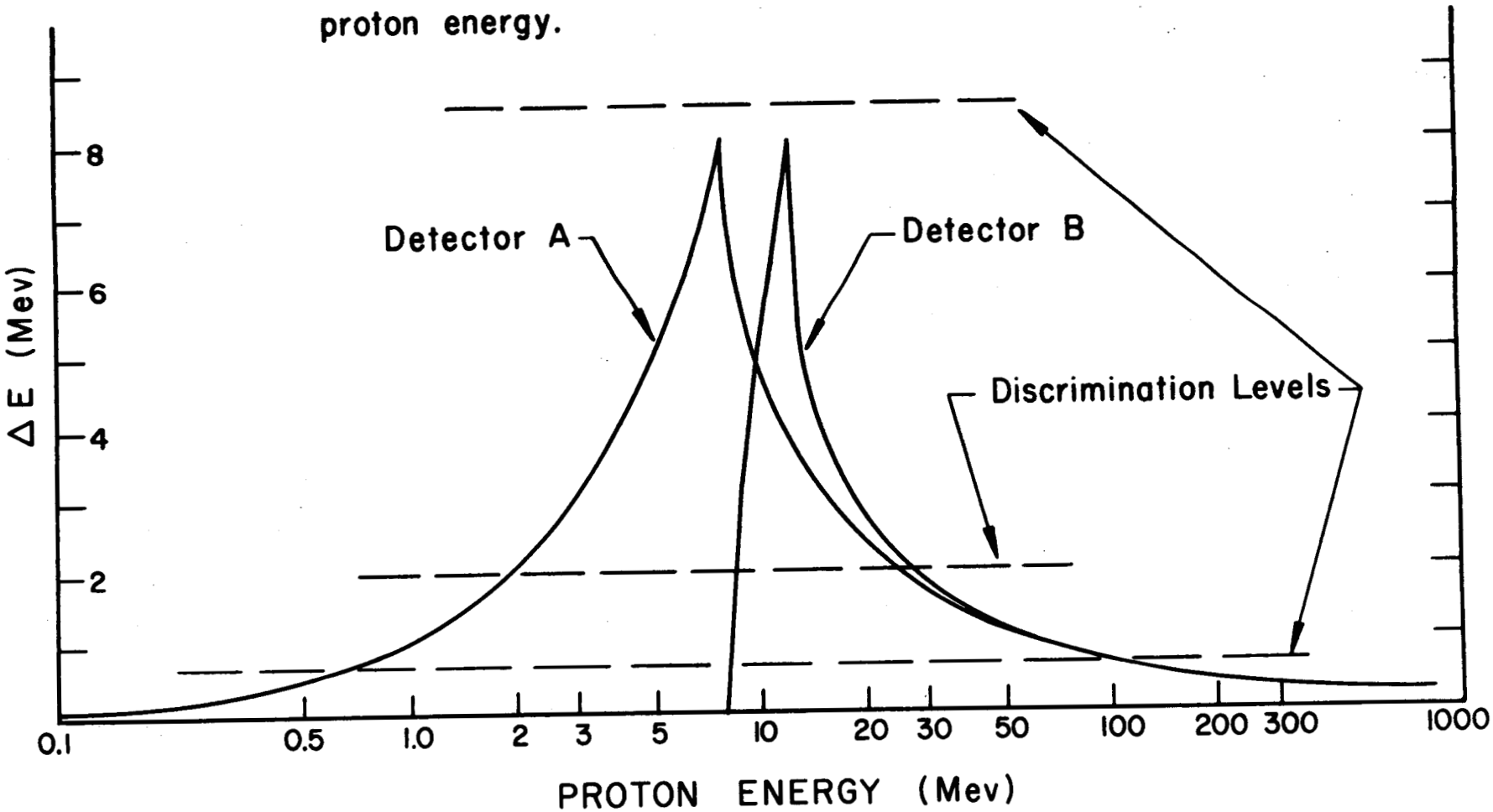

Fig. 9